Momentum-Density Studies of Some Compounds with Triatomic Linear Anions*

R. O. Horenian and W. Weyrich

Fakultät für Chemie, Universität Konstanz, Konstanz, Fed. Rep. of Germany

Z. Naturforsch. **48a**, 325–333 (1993); received January 28, 1993

High-purity powder samples of lithium and sodium azide (LiN_3, NaN_3), cyanate (LiOCN, NaOCN) and hydrogen fluoride (LiFHF, NaFHF) were studied by means of 59.54 keV Compton spectroscopy. The measured isotropic Compton profiles were corrected for multiple scattering and transformed to spherically averaged reciprocal form factors $B^a(s)$.

The experimental results are compared with theoretical reciprocal form factors obtained from Hartree–Fock calculations with different types of basis sets (Gaussian- and Slater-type orbitals, with and without polarisation functions) both for the free ions and for several kinds of clusters. The importance of intraionic and interionic interaction for the description of chemical bonding in these compounds is pointed out and discussed.

Key words: Compton spectroscopy; Azides; Hydrogen fluorides; Cyanates; Ionic crystals.

1. Introduction

Compton spectroscopy provides a powerful and sensitive experimental tool in studying the electronic momentum distribution in atoms, molecules and solids, as in the impulse approximation [1, 2] it yields a complete one-dimensional electron momentum distribution in the scatterer. Some effort has been expended to correlate chemical properties with the spherically averaged one-electron momentum density $\pi(\boldsymbol{p})$ and the isotropic Compton profile $J(\boldsymbol{q})$ (see, e.g., [3]). The main effect of chemical bonding is the broadening of $\pi(\boldsymbol{p})$ and $J(\boldsymbol{q})$ owing to the virial theorem and the plane-wave-type modulation by the interference between atoms. Within the context of the impulse approximation, the shape of the measured Compton band reflects the one-dimensional projection of the total electron momentum density onto a line $\boldsymbol{q}$ in the direction of the scattering vector of the experiment. When the target system studied is randomly oriented (gases, liquids, powders) the momentum density $\pi(\boldsymbol{p})$ seen by the experiment is spherically symmetrical, $\pi(p) = \langle \pi(\boldsymbol{p}) \rangle_\Omega$ and the quantity measured is the isotropic (spherically averaged) Compton profile

$$J(p_z) = \int_{p_x} \int_{p_y} \pi(p)\, \mathrm{d}p_x\, \mathrm{d}p_y \tag{1}$$

or, in spherical momentum coordinates,

$$J(q) = 2\pi \int_{|q|}^{\infty} \pi(p)\, p\, \mathrm{d}p\,. \tag{2}$$

Although comparison of experimental and theoretical results can be done at this level, we prefer using the reciprocal form factor, $B^a(\boldsymbol{s})$. It is a function defined as the 3D Fourier transform of the electron momentum density $\pi(\boldsymbol{p})$ as well as the 1D Fourier transform of the Compton profile $J(\boldsymbol{q})$ (see also [4] and the references therein):

$$\begin{aligned} B(\boldsymbol{s}) &= \int_{-\infty}^{\infty}\int\int \pi(\boldsymbol{p})\, e^{-i\boldsymbol{p}\boldsymbol{s}}\, \mathrm{d}\boldsymbol{p} \\ &= \int_{-\infty}^{\infty} J(\boldsymbol{q})\, e^{-i\boldsymbol{q}\boldsymbol{s}}\, \mathrm{d}q \quad (\boldsymbol{q} \parallel \boldsymbol{s}) \end{aligned} \tag{3}$$

or, in the spherical average,

$$\begin{aligned} B(s) &= 4\pi \int_{0}^{\infty} \pi(p)\, j_0(p\,s)\, p^2\, \mathrm{d}p \\ &= \int_{-\infty}^{\infty} J(q)\, e^{-iqs}\, \mathrm{d}q \end{aligned} \tag{4}$$

The reciprocal form factor is the position-space representation of $\pi(\boldsymbol{p})$ and $J(\boldsymbol{q})$ and can also be expressed as the sum of orbital autocorrelation functions

* Presented at the Sagamore X Conference on Charge, Spin and Momentum Densities, Konstanz, Fed. Rep. of Germany, September 1–7, 1991.

Reprint requests to Prof. Dr. Dr. h.c. Wolf Weyrich, Lehrstuhl für Physikalische Chemie I, Fakultät für Chemie, Universität Konstanz, Postfach 55 60, D-W-7750 Konstanz, Fed. Rep. of Germany.

0932-0784 / 93 / 0100-0325 $ 01.30/0. – Please order a reprint rather than making your own copy.

weighted by the occupation numbers n_j,

$$B(s) = \sum_j n_j \int_{-\infty}^{\infty} \int \int \psi_j(r) \psi_j^*(r+s) \, dr . \quad (5)$$

Most methods of calculating theoretical reciprocal form factors that start from the position-space wave function of an electronic system make use of the relationship in (5).

2. Experiment

Four of the six substances that we have analysed had to be synthesised (LiN_3, LiOCN, LiFHF and NaFHF), the other two (NaN_3 and NaOCN) were purchased; all except sodium azide had to be purified before use. Only a *résumé* of the synthesis and purification of the substances is given here; for more detailed information see [5].

Lithium azide was prepared by the method described by Hoth et al. [6]. After sixfold recrystallisation from ethanol/ether (1:9 by volume) the substance reached a purity of 99.7%. Sodium azide was purchased from E. Merck, Darmstadt. All analysed samples of the product showed a purity exceeding 99.5%. The purity of the azides was determined by Mohr titration as described in [7], using the special indicator (a mixture of potassium chromate and dichromate) recommended by Belcher et al. [8].

The synthesis of lithium hydrogen fluoride proved to be rather difficult, and several methods had to be used before we succeeded. We found the compound to be highly unstable (even at room temperature it rapidly decomposes into LiF and HF), in accordance with the statements of Kruh et al. [9]. The synthesis was performed with the method described by Ludman et al. [10], using a 70% solution of hydrogen fluoride in a 14-fold excess. The resultant LiFHF was flushed with dry nitrogen at room temperature for 15 minutes to drive off excess HF and water. According to our observations, it is not possible to dry the substance at 95 °C without significant loss of HF. Sodium hydrogen fluoride was prepared without considerable difficulties by a similar method, the substance being much more stable than the lithium salt. The purity of the hydrogen fluorides was determined by acidimetric titration with a 0.1 *n* NaOH solution.

Sodium cyanate was purchased from Janssen Chimica. It is well known that cyanates undergo slow hydrolysis yielding ammonium and carbonate ions and that they have to be dried thoroughly to avoid partial decomposition on storage. Pure NaOCN can be obtained by *careful* recrystallisation from water by the method described by Scattergood [11]. Qualitative tests for carbonate, ammonium, urea and cyanide were negative. Lithium cyanate is an almost unknown substance and only rarely mentioned in literature so far. The synthesis was therefore carried out using the same method as for NaOCN and gave good results (see [5] for details concerning preparation and purification of LiOCN). The purity of the cyanates was determined by a gravimetric method; cyanate is precipitated by $AgNO_3$ from dilute nitric-acid or neutral solution (Duval, [12]).

The Compton measurements in this work were performed with a spectrometer built by Bachmann [13] and modified by Haas (for a detailed description of the spectrometer see [14]), employing an annular ^{241}Am source (primary photon-energy 59.537 keV) of 5 Ci activity. Photons scattered under an angle of 163.5° were detected. All spectra were recorded under vacuum (0.2–0.4 mbar). Because of its instability, the LiFHF spectra had to be measured at temperatures between -50 and -60 °C using a special sample holder. Chemical analysis as well as (except for LiFHF, where we had to rely on the chemical analysis alone) weighing of the pressed powder sample before and after the measurement guarantee for the high purity (> 99%) of the examined specimens.

The scattered photons were analysed with an intrinsic-Ge detector (Princeton Gamma-Tech), the signals amplified, shaped and finally registered by a multichannel-analyser. All spectra consisted of 4096 channels (channel width 20 eV), at least 21,000,000 photons for the spectra of the lithium salts and 41,000,000 photons for the spectra of the sodium salts were collected. The resulting standard deviation of $B^a(s)$ was thus less than 0.005 electrons for all measurements. The purely Gaussian resolution function of the experiment had a full width at half maximum $\Delta q_{FWHM} = 0.604\, p_0$ ($p_0 = 1$ Dumond $= 1.99289 \cdot 10^{-24}$ kg m s^{-1}).

The various steps in processing the recorded data have been described earlier (see, e.g., [4]). Because of the convolution of the Compton profile $J(q)$ with the experimental resolution function to $J^c(q)$, the reciprocal form factor obtained is attenuated by the multiplicative function

$$G(s) = \exp[-(s/2.9177\ \text{Å})^2] \quad (6)$$

to $B^a(s)$. A correction for multiple scattering was done by extrapolating the measured $B^a(s)$ values to zero sample thickness.

3. Calculation of Theoretical Data

Calculations of theoretical reciprocal form factors were performed, using both Gauss-type and Slater-type orbitals (GTOs and STOs). For the calculations with GTOs we used the program GAMESS (General Atomic and Molecular Electronic Structure System) described by M. W. Schmidt et al. [15] and M. Dupuis et al. [16]. For a few systems, calculations with the program CRYSTAL 88 (a Hartree-Fock SCF program for periodic systems) of Pisani et al. [17, 18] were also performed. From the obtained HF-SCF molecular wave functions, $B^a(s)$ values were calculated by the autocorrelation relationship of (5). For all the three anions, calculations using the program BVSSM (see [5]) were performed. This program uses the Fourier-transformed STOs for calculating the spherically averaged momentum density; the $B^a(s)$ is then obtained by Fourier-Hankel transformation of the isotropic momentum density (see (4)).

4. Results and Discussion

For the cations Li^+ and Na^+, calculations for both the free ions and for some arrangements of ions using basis sets of different quality were performed. The reciprocal form factors for lithium are shown in Figure 1. Curve **a** is the $B^a(s)$ of a lithium atom (we used the STO basis set of Clementi et al. [19]), the curves **b**–**e** are obtained from different GTO basis sets implemented in GAMESS, curve **f** is for a basis set of Clementi et al. [19] again, this time for Li^+. We had some difficulties in getting closer than $0.2\,E_h$ ($E_h = 1$ Hartree $= 27.212$ eV $= 4.359828 \cdot 10^{-18}$ J) to the Hartree-Fock limit for lithium, even with the best basis set. Significant differences between curve **b** (MIDI basis set [20]) and **d** (3-21 G basis set [21]) on the one hand and **c** (DH basis set [22]) and **e** (6-21 G basis set [21]) on the other, can clearly be seen. Basis sets that differ only slightly in the convergence energy may still have quite different reciprocal form factors.

A similar effect is observed in the case of sodium. Figure 2 shows a comparison of reciprocal form factors obtained by starting from the same basis sets as in Figure 1.

Four of the six investigated substances have rhombohedral (trigonal) crystal structures (LiFHF [23], NaN_3 [24] and NaFHF [25] belong to spacegroup D^5_{3d}, $R\bar{3}m$, No. 166, whereas NaOCN [26] – because of the less symmetric anion – belongs to spacegroup C^5_{3v}, R3m, No. 160). The triatomic linear anions are oriented parallel to the C_3-axes of the crystal structure in all four compounds. Lithium azide is monoclinic (spacegroup C^3_{2h}, C2/m, No. 12 [24]); the unit cell of lithium cyanate is also monoclinic, as determined in [5].

For the less symmetric monoclinic systems LiN_3 and LiOCN, the influence of the quality of the basis set on the calculated theoretical reciprocal form factors $B^a(s)$ was studied in comparison to the experiment. The $B^a(s)$ for LiN_3 and LiOCN were obtained by superposition of separate anion and cation contributions.

Figure 3 shows the comparison of the data for LiOCN; curve **a** is the reciprocal form factor for separate (i.e. noninteracting) atoms, obtained from the basis set of Clementi et al. [19], curve **b** is the experiment. The curves **c**–**e** were calculated starting from different basis sets implemented in the program GAMESS (MINI, MIDI and DH) for the NCO^- anion; the cation contribution is the same in all cases (DH basis set for Li^+). Curve **f** was obtained from the double-zeta-plus-polarisation (DZ + P) STO basis set of McLean et al. [27].

The comparison of theoretical and experimental reciprocal form factors for LiN_3 is shown in Figure 4. GAMESS-implemented basis sets were used for the N_3^- anion again; the Li^+ contribution to the reciprocal form factor is the same as in Figure 3. Similar effects as in the case of LiOCN were found. The MINI and MIDI basis sets predict a too low minimum for the $B^a(s)$. The position of this minimum as well as the depth changes when using better basis sets (DH). Only qualitative agreement between theory and experiment can be reached in the case of LiN_3; for LiOCN the agreement is even poorer.

For the substances with rhombohedral crystal structures (see above), several types of symmetry-adapted clusters consisting of three or more anions or cations as well as of mixtures of anions and cations were used for the calculations.

Figure 5 shows the comparison of experimental and theoretical curves for LiFHF. The influence of the quality of the wave functions used can again be clearly seen when comparing curve **c** (obtained from a MIDI GTO basis set) with curve **d** (DH). The reciprocal form factors of the curves **e** and **f** were calculated with a basis set owing to Kistenmacher et al. [28], with a MINI basis set for hydrogen in curve **e** and DH for

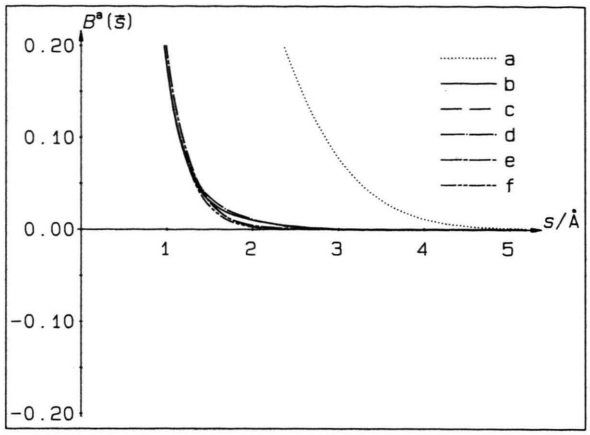

Fig. 1. Theoretical reciprocal form factor $B^a(s)$, attenuated by the experimental resolution. a) Lithium atom, basis set of Clementi et al. [19], b) Li^+, MIDI basis set [20], c) Li^+, DH bases set [22], d) Li^+, 3-21 G basis set [21], e) Li^+, 6-21 G basis set [21] and f) Li^+, basis set of Clementi et al. [19]. See Table 1 for the $B^a(s)$ values.

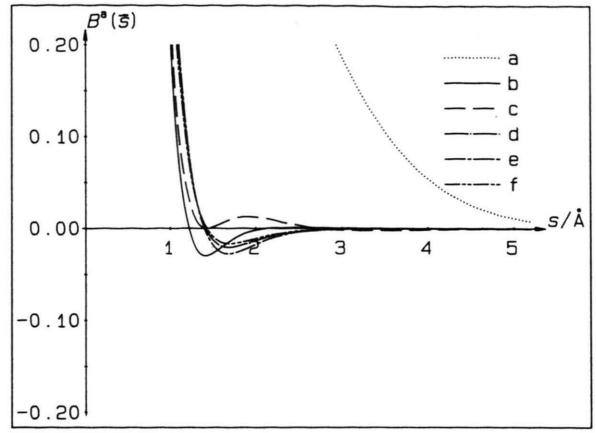

Fig. 2. Theoretical reciprocal form factor $B^a(s)$ for sodium, attenuated by the experimental resolution. a) Sodium atom, basis set of Clementi et al. [19], b) Na^+, MIDI basis set [20], c) Na^+, 3-21 G basis set [31], d) Na^+, MC basis set [30], e) Na^+, 6-21 G basis set [31] and f) Na^+, basis set of Clementi et al. [19].

Table 1. Theoretical reciprocal form factor $B^a(s)$ for lithium. See also Figure 1.

s/Å	$B^a(s)$					
	(a)	(b)	(c)	(d)	(e)	(f)
0.00	3.000	2.000	2.000	2.000	2.000	2.000
0.15	2.809	1.824	1.823	1.823	1.823	1.819
0.30	2.387	1.437	1.435	1.435	1.436	1.423
0.45	1.933	1.027	1.027	1.025	1.028	1.008
0.60	1.542	0.685	0.688	0.681	0.689	0.666
0.75	1.239	0.429	0.440	0.425	0.440	0.417
0.90	1.013	0.253	0.271	0.252	0.271	0.251
1.05	0.845	0.145	0.162	0.146	0.162	0.146
1.20	0.716	0.082	0.094	0.085	0.094	0.083
1.35	0.614	0.048	0.054	0.052	0.053	0.046
1.50	0.529	0.030	0.030	0.034	0.029	0.025
1.65	0.455	0.021	0.016	0.024	0.016	0.013
1.80	0.390	0.015	0.009	0.017	0.009	0.007
1.95	0.331	0.011	0.005	0.012	0.005	0.003
2.10	0.278	0.008	0.002	0.009	0.003	0.002
2.25	0.232	0.006	0.001	0.006	0.002	0.001
2.40	0.191	0.004	0.001	0.004	0.001	0.000
2.55	0.155	0.003	0.000	0.002	0.001	0.000
2.70	0.124	0.002	0.000	0.001	0.000	
2.85	0.099	0.001		0.000	0.000	
3.00	0.077	0.000		0.000		
3.15	0.060	0.000				
3.30	0.046					
3.45	0.035					
3.60	0.026					
3.75	0.019					
3.90	0.014					
4.05	0.010					
4.20	0.007					
4.35	0.005					
4.50	0.003					
4.65	0.002					
4.80	0.002					

Table 2. Theoretical reciprocal form factor $B^a(s)$ for sodium. See also Figure 2.

s/Å	$B^a(s)$					
	(a)	(b)	(c)	(d)	(e)	(f)
0.00	11.000	10.000	10.000	10.000	10.000	10.000
0.15	8.649	7.649	7.656	7.656	7.658	7.640
0.30	6.119	5.114	5.138	5.138	5.149	5.099
0.45	4.249	3.266	3.296	3.290	3.310	3.237
0.60	2.892	1.916	1.940	1.966	1.990	1.911
0.75	1.974	0.997	1.020	1.089	1.111	1.043
0.90	1.391	0.431	0.458	0.553	0.571	0.521
1.05	1.038	0.133	0.163	0.250	0.263	0.232
1.20	0.826	0.008	0.039	0.092	0.097	0.085
1.35	0.698	−0.027	0.003	0.017	0.016	0.017
1.50	0.614	−0.027	0.002	−0.013	−0.019	−0.009
1.65	0.553	−0.017	0.008	−0.021	−0.028	−0.016
1.80	0.502	−0.008	0.012	−0.019	−0.025	−0.015
1.95	0.456	−0.003	0.013	−0.014	−0.019	−0.012
2.10	0.412	0.000	0.011	−0.010	−0.013	−0.009
2.25	0.369	0.001	0.008	−0.007	−0.008	−0.006
2.40	0.328	0.001	0.005	−0.004	−0.005	−0.004
2.55	0.289	0.001	0.002	−0.003	−0.003	−0.002
2.70	0.252	0.001	0.000	−0.002	−0.002	−0.001
2.85	0.218	0.001	−0.001	−0.001	−0.001	−0.001
3.00	0.187	0.000	−0.002	−0.001	−0.001	0.000
3.15	0.159	0.000	−0.002	0.000	0.000	0.000
3.30	0.134		−0.002	0.000	0.000	
3.45	0.112		−0.002			
3.60	0.093		−0.002			
3.75	0.076		−0.002			
3.90	0.062		−0.001			
4.05	0.050		−0.001			
4.20	0.040		−0.001			
4.35	0.032		−0.001			
4.50	0.025		0.000			
4.65	0.020		0.000			
4.80	0.015					

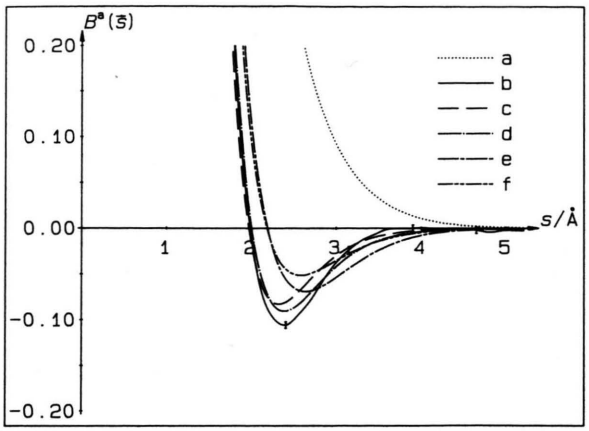

Fig. 3. Comparison between experimental and theoretical $B^a(s)$ for LiOCN. a) Superposition of noninteracting atoms, basis set of Clementi et al. [19] for all atoms (Li, O, C, N), b) experimental reciprocal form factor, c) theoretical $B^a(s)$, Li^+: DH basis set [22], NCO^-: MINI basis set [20], d) theoretical $B^a(s)$, Li^+: DH basis set [22], NCO^-: MIDI basis set [20], e) theoretical $B^a(s)$, Li^+: DH basis set [22], NCO^-: DH basis set [22], f) theoretical $B^a(s)$, Li^+: DH basis set [22], NCO^-: basis set of McLean et al. [27].

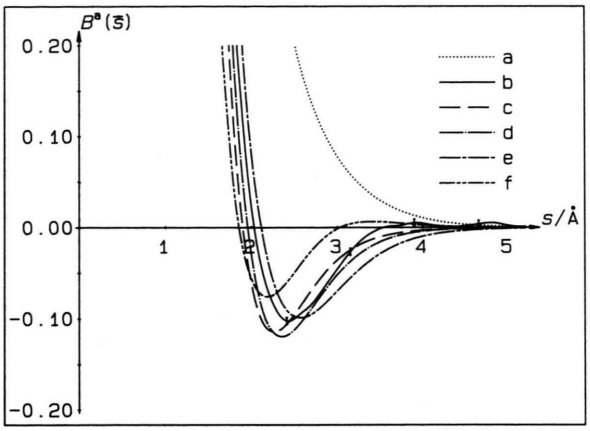

Fig. 4. Comparison between experimental and theoretical $B^a(s)$ for LiN_3. a) Superposition of noninteracting atoms, basis set of Clementi et al. for all atoms [19], b) experimental reciprocal form factor, c) theoretical $B^a(s)$, Li^+: DH basis set [22], N_3^-: MINI basis set [20], d) theoretical $B^a(s)$, Li^+: DH basis set [22], N_3^-: MIDI basis set [20], e) theoretical $B^a(s)$, Li^+: DH basis set [22], N_3^-: DH basis set [22], f) theoretical $B^a(s)$, Li^+: DH basis set [22], N_3^-: basis set of McLean et al. [27].

Table 3. Reciprocal form factor of LiOCN, experiment vs. theory. See also Figure 3.

s/Å	$B^a(s)$					
	(a)	(b)	(c)	(d)	(e)	(f)
0.00	24.008	23.917	24.000	24.000	24.000	23.991
0.15	20.748	21.071	20.725	20.783	20.767	20.697
0.30	16.270	16.485	16.114	16.263	16.283	16.194
0.45	12.839	12.865	12.507	12.715	12.776	12.664
0.60	10.141	9.915	9.642	9.872	9.941	9.816
0.75	7.922	7.465	7.230	7.455	7.544	7.425
0.90	6.097	5.406	5.218	5.419	5.540	5.434
1.05	4.626	3.767	3.604	3.775	3.929	3.833
1.20	3.469	2.501	2.370	2.512	2.693	2.599
1.35	2.578	1.573	1.465	1.581	1.777	1.687
1.50	1.905	0.914	0.831	0.923	1.119	1.040
1.65	1.403	0.473	0.413	0.481	0.662	0.599
1.80	1.032	0.188	0.156	0.201	0.356	0.312
1.95	0.760	0.025	0.012	0.037	1.161	0.135
2.10	0.560	−0.063	−0.057	−0.048	0.043	0.033
2.25	0.414	−0.097	−0.081	−0.083	−0.023	−0.021
2.40	0.307	−0.106	−0.081	−0.091	−0.056	−0.045
2.55	0.227	−0.095	−0.070	−0.083	−0.068	−0.051
2.70	0.169	−0.078	−0.055	−0.070	−0.068	−0.049
2.85	0.125	−0.056	−0.041	−0.055	−0.062	−0.043
3.00	0.092	−0.037	−0.030	−0.042	−0.053	−0.035
3.15	0.068	−0.023	−0.021	−0.030	−0.044	−0.028
3.30	0.050	−0.013	−0.014	−0.022	−0.034	−0.021
3.45	0.036	−0.007	−0.010	−0.015	−0.026	−0.015
3.60	0.026	−0.001	−0.007	−0.010	−0.019	−0.011
3.75	0.019	0.000	−0.004	−0.007	−0.014	−0.008
3.90	0.013	0.000	−0.003	−0.004	−0.010	−0.005
4.05	0.009	0.000	−0.002	−0.003	−0.007	−0.004
4.20	0.007	−0.002	−0.001	−0.002	−0.005	−0.003
4.35	0.005	0.000	−0.001	−0.001	−0.003	−0.002
4.50	0.003	−0.001	0.000	−0.001	−0.002	−0.001
4.65	0.002	−0.002	0.000	0.000	−0.001	−0.001
4.80	0.001	−0.004		0.000	−0.001	0.000

Table 4. Reciprocal form factor of LiN_3, experiment vs. theory. See also Figure 4.

s/Å	$B^a(s)$					
	(a)	(b)	(c)	(d)	(e)	(f)
0.00	24.000	23.916	24.000	24.000	24.000	23.998
0.15	20.760	21.112	20.767	20.830	20.815	20.588
0.30	16.274	16.553	16.202	16.370	16.392	15.975
0.45	12.850	12.984	12.670	12.915	12.979	12.314
0.60	10.142	10.087	9.868	10.156	10.216	9.295
0.75	7.884	7.656	7.457	7.757	7.838	6.742
0.90	6.005	5.590	5.402	5.690	5.805	4.657
1.05	4.485	3.931	3.727	3.989	4.132	3.045
1.20	3.294	2.638	2.431	2.661	2.827	1.870
1.35	2.388	1.689	1.477	1.669	1.851	1.060
1.50	1.716	1.007	0.810	0.960	1.148	0.535
1.65	1.227	0.546	0.373	0.482	0.661	0.218
1.80	0.877	0.245	0.108	0.181	0.337	0.042
1.95	0.629	0.065	−0.035	0.006	0.131	−0.042
2.10	0.454	−0.037	−0.098	−0.082	0.008	−0.073
2.25	0.331	−0.084	−0.114	−0.115	−0.059	−0.074
2.40	0.244	−0.102	−0.106	−0.118	−0.090	−0.060
2.55	0.181	−0.095	−0.087	−0.106	−0.099	−0.042
2.70	0.136	−0.083	−0.067	−0.088	−0.094	−0.024
2.85	0.102	−0.064	−0.049	−0.068	−0.083	−0.010
3.00	0.077	−0.045	−0.035	−0.051	−0.069	−0.001
3.15	0.058	−0.027	−0.024	−0.037	−0.055	0.004
3.30	0.044	−0.012	−0.017	−0.026	−0.042	0.006
3.45	0.033	−0.003	−0.011	−0.018	−0.032	0.007
3.60	0.024	0.001	−0.008	−0.012	−0.023	0.006
3.75	0.018	0.003	−0.005	−0.008	−0.017	0.005
3.90	0.013	0.005	−0.004	−0.005	−0.012	0.003
4.05	0.009	0.004	−0.002	−0.003	−0.008	0.002
4.20	0.007	0.001	−0.002	−0.002	−0.006	0.002
4.35	0.005	0.001	−0.001	−0.001	−0.004	0.001
4.50	0.003	0.002	−0.001	−0.001	−0.003	0.001
4.65	0.002	0.004	0.000	−0.001	−0.002	0.000
4.80	0.002	0.005	0.000	0.000	−0.001	0.000

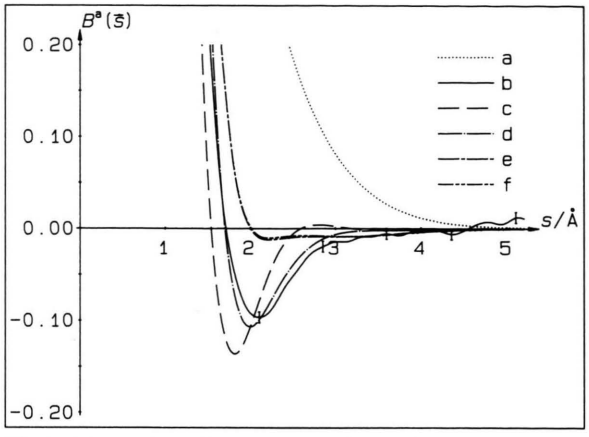

Fig. 5. Comparison between experimental and theoretical $B^a(s)$ for LiFHF. a) Superposition of noninteracting atoms, basis set of Clementi et al. for all atoms [19], b) experimental reciprocal form factor, c) theoretical $B^a(s)$, Li^+: DH basis set [22], FHF^-: MIDI basis set [20], d) theoretical $B^a(s)$, Li^+: DH basis set [22], FHF^-: DH basis set [22], e) theoretical $B^a(s)$, Li^+: DH basis set [22], FHF^-: basis set of Kistenmacher et al. [28] for fluorine and MINI basis set [22] for hydrogen, f) same as e), but DH basis set ([22]) on hydrogen.

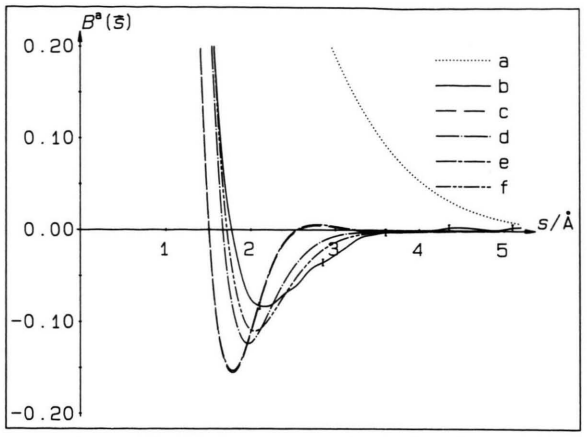

Fig. 6. Comparison between experimental and theoretical $B^a(s)$ for NaFHF. a) Superposition of noninteracting atoms, basis set of Clementi et al. [19] for all atoms, b) experimental reciprocal form factor, c) theoretical $B^a(s)$, Na^+: MIDI basis set [20] FHF^-: MIDI basis set [20], d) theoretical $B^a(s)$, Na^+: MC basis set [30], FHF^-: DH basis set [22], e) theoretical $B^a(s)$, Na^+ contribution from a cluster consisting of 3 Na^+ cations with MIDI basis set [20], and 3 FHF^- anions, also MIDI basis set, f) same as e), but with MC basis set [30] on sodium and DH basis set on FHF^-.

Table 5. Reciprocal form factor of LiFHF, experiment vs. theory. See also Figure 5.

s/Å	$B^a(s)$					
	(a)	(b)	(c)	(d)	(e)	(f)
0.00	22.000	21.856	22.000	22.000	22.000	22.000
0.15	18.528	19.030	18.576	18.566	18.566	18.566
0.30	14.218	14.699	14.223	14.282	14.294	14.294
0.45	10.792	11.280	10.720	10.832	10.867	10.867
0.60	7.993	8.405	7.757	7.952	8.017	8.016
0.75	5.772	6.080	5.324	5.603	5.697	5.696
0.90	4.095	4.215	3.422	3.768	3.889	3.887
1.05	2.880	2.817	2.008	2.396	2.538	2.535
1.20	2.027	1.052	1.028	1.413	1.566	1.564
1.35	1.441	0.551	0.410	0.742	0.900	0.899
1.50	1.041	0.241	0.065	0.311	0.469	0.469
1.65	0.768	0.052	−0.093	0.060	0.211	0.211
1.80	0.579	−0.042	−0.136	−0.064	0.072	0.073
1.95	0.445	−0.086	−0.119	−0.105	0.010	0.011
2.10	0.347	−0.096	−0.079	−0.099	−0.010	−0.008
2.25	0.273	−0.087	−0.041	−0.076	−0.012	−0.010
2.40	0.216	−0.064	−0.016	−0.052	−0.010	−0.009
2.55	0.170	−0.045	−0.002	−0.033	−0.009	−0.008
2.70	0.134	−0.028	0.003	−0.020	−0.009	−0.008
2.85	0.105	−0.020	0.004	−0.011	−0.009	−0.008
3.00	0.081	−0.014	0.002	−0.006	−0.009	−0.009
3.15	0.062	−0.014	0.000	−0.004	−0.009	−0.009
3.30	0.047	−0.009	−0.001	−0.002	−0.008	−0.008
3.45	0.036	−0.008	−0.002	−0.002	−0.008	−0.008
3.60	0.026	−0.006	−0.002	−0.002	−0.007	−0.007
3.75	0.019	−0.008	−0.002	−0.002	−0.005	−0.006
3.90	0.014	−0.003	−0.001	−0.002	−0.004	−0.005
4.05	0.010	−0.002	−0.001	−0.001	−0.003	−0.004
4.20	0.007	−0.002	−0.001	−0.001	−0.003	−0.003
4.35	0.005	−0.006	0.000	−0.001	−0.002	−0.002
4.50	0.004	−0.002	0.000	−0.001	−0.001	−0.001
4.65	0.002	0.005		0.000	−0.001	−0.001
4.80	0.002	0.007		0.000	−0.001	−0.001

Table 6. Reciprocal form factor of NaFHF, experiment vs. theory. See also Figure 6.

s/Å	$B^a(s)$					
	(a)	(b)	(c)	(d)	(e)	(f)
0.00	30.000	29.707	30.000	30.000	30.000	30.000
0.15	24.368	25.059	24.405	24.401	24.405	24.399
0.30	17.949	18.622	17.909	17.990	17.909	17.972
0.45	13.109	13.831	12.964	13.098	12.964	13.069
0.60	9.343	9.966	8.988	9.232	8.988	9.197
0.75	6.507	7.022	5.882	6.252	5.881	6.222
0.90	4.473	4.757	3.579	4.048	3.579	4.029
1.05	3.073	3.131	1.974	2.480	1.975	2.482
1.20	2.137	1.956	0.935	1.404	0.936	1.430
1.35	1.524	1.165	0.321	0.698	0.323	0.742
1.50	1.126	0.297	0.002	0.263	0.004	0.314
1.65	0.866	0.088	−0.131	0.019	−0.128	0.068
1.80	0.691	−0.015	−0.155	−0.093	−0.153	−0.057
1.95	0.570	−0.067	−0.126	−0.124	−0.125	−0.104
2.10	0.480	−0.083	−0.081	−0.110	−0.079	−0.108
2.25	0.410	−0.081	−0.040	−0.082	−0.039	−0.092
2.40	0.353	−0.069	−0.014	−0.056	−0.013	−0.071
2.55	0.304	−0.059	−0.001	−0.035	0.001	−0.050
2.70	0.262	−0.043	0.004	−0.021	0.005	−0.034
2.85	0.224	−0.036	0.004	−0.012	0.005	−0.022
3.00	0.191	−0.027	0.003	−0.007	0.004	−0.014
3.15	0.161	−0.018	0.001	−0.004	0.001	−0.008
3.30	0.135	−0.008	−0.001	−0.003	0.000	−0.005
3.45	0.113	−0.005	−0.002	−0.002	−0.001	−0.003
3.60	0.093	−0.002	−0.002	−0.002	−0.002	−0.002
3.75	0.077	−0.002	−0.002	−0.002	−0.002	−0.001
3.90	0.062	−0.001	−0.001	−0.002	−0.001	−0.001
4.05	0.050	0.000	−0.001	−0.001	−0.001	−0.001
4.20	0.040	0.001	−0.001	−0.001	−0.001	−0.001
4.35	0.032	0.003	0.000	−0.001	0.000	0.000
4.50	0.025	0.004	0.000	−0.001	0.000	0.000
4.65	0.020	0.002		−0.001		
4.80	0.016	0.001		0.000		

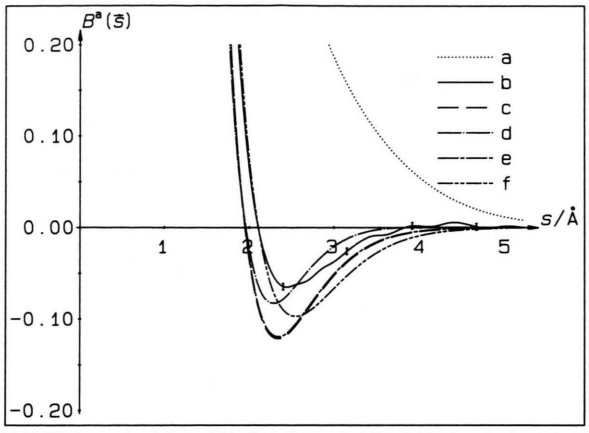

Fig. 7. Comparison between experimental and theoretical $B^a(s)$ for NaN_3. a) Superposition of noninteracting atoms, basis set of Clementi et al. for all atoms [19], b) experimental reciprocal form factor, c) theoretical $B^a(s)$, Na^+: MIDI basis set [20], N_3^-: MIDI basis set [20], d) theoretical $B^a(s)$, Na^+ contribution from a cluster consisting of $3\,Na^+$ cations with MIDI basis set [20], and $3\,N_3^-$ anions, also MIDI basis set, e) theoretical $B^a(s)$ of a mixed cluster consisting of $3\,Na^+$ with MIDI basis set [20], and $3\,N_3^-$, also MIDI basis set, f) same as e), only with MC basis set ([30]) on sodium and DH basis set on N_3^-.

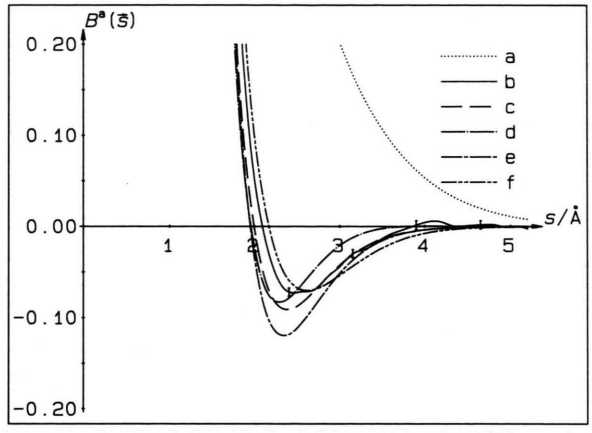

Fig. 8. Comparison between experimental and theoretical $B^a(s)$ for NaOCN. a) Superposition of noninteracting atoms, basis set of Clementi et al. for all atoms [19], b) experimental reciprocal form factor, c) theoretical $B^a(s)$, Na^+: MIDI basis set [20], NCO^-: MIDI basis set [20], d) theoretical $B^a(s)$, Na^+ contribution from a cluster consisting of $3\,Na^+$ cations, MIDI basis set [20], and $3\,NCO^-$ anions, also MIDI basis set, e) theoretical $B^a(s)$ mixed cluster consisting of $3\,Na^+$: MIDI basis set [20], and $3\,NCO^-$, also MIDI basis set, f) same as e), but with MC basis set [30] on sodium and DH basis set on NCO^-.

Table 7. Reciprocal form factor of NaN_3, experiment vs. theory. See also Figure 7.

s/Å	$B^a(s)$					
	(a)	(b)	(c)	(d)	(e)	(f)
0.00	32.000	31.770	32.000	32.000	32.000	32.000
0.15	26.600	27.099	26.661	26.656	26.661	26.654
0.30	20.006	20.373	20.063	20.025	20.063	20.111
0.45	15.167	15.429	15.170	15.094	15.171	15.260
0.60	11.492	11.534	11.401	11.296	11.402	11.515
0.75	8.619	8.482	8.331	8.215	8.333	8.509
0.90	6.384	6.025	5.862	5.749	5.865	6.105
1.05	4.678	4.162	3.970	3.868	3.973	4.238
1.20	3.405	2.760	2.583	2.492	2.586	2.841
1.35	2.472	1.763	1.594	1.515	1.597	1.829
1.50	1.801	1.059	0.908	0.847	0.911	1.119
1.65	1.325	0.596	0.452	0.413	0.455	0.637
1.80	0.990	0.288	0.165	0.149	0.167	0.320
1.95	0.754	0.107	−0.001	0.005	0.001	0.120
2.10	0.588	0.001	−0.086	−0.062	−0.083	0.003
2.25	0.469	−0.046	−0.118	−0.082	−0.116	−0.061
2.40	0.381	−0.065	−0.120	−0.078	−0.118	−0.090
2.55	0.315	−0.062	−0.108	−0.064	−0.106	−0.097
2.70	0.264	−0.058	−0.089	−0.047	−0.088	−0.092
2.85	0.222	−0.046	−0.070	−0.032	−0.068	−0.081
3.00	0.187	−0.037	−0.052	−0.021	−0.051	−0.067
3.15	0.157	−0.026	−0.038	−0.012	−0.037	−0.053
3.30	0.132	−0.015	−0.027	−0.007	−0.026	−0.040
3.45	0.110	−0.009	−0.018	−0.003	−0.017	−0.030
3.60	0.091	−0.008	−0.012	−0.001	−0.012	−0.022
3.75	0.075	−0.002	−0.008	0.000	−0.008	−0.015
3.90	0.061	0.002	−0.005	0.000	−0.005	−0.011
4.05	0.050	0.001	−0.003		−0.003	−0.007
4.20	0.040	0.002	−0.002		−0.002	−0.005
4.35	0.032	0.006	−0.001		−0.001	−0.003
4.50	0.025	0.004	−0.001		−0.001	−0.002
4.65	0.020	0.001	−0.001		0.000	−0.002
4.80	0.015	−0.001	0.000		0.000	−0.001

Table 8. Reciprocal form factor of NaOCN, experiment vs. theory. See also Figure 8.

s/Å	$B^a(s)$					
	(a)	(b)	(c)	(d)	(e)	(f)
0.00	32.008	31.771	32.000	32.000	32.000	32.000
0.15	26.588	27.056	26.613	26.559	26.592	26.604
0.30	20.002	20.275	19.953	19.850	19.873	19.996
0.45	15.156	15.277	14.966	14.816	15.005	15.049
0.60	11.491	11.341	11.113	10.949	11.108	11.228
0.75	8.657	8.297	8.025	7.922	8.173	8.203
0.90	6.475	5.877	5.588	5.583	5.771	5.829
1.05	4.819	4.054	3.755	3.826	3.978	4.023
1.20	3.579	2.685	2.434	2.547	2.499	2.696
1.35	2.662	1.710	1.507	1.641	1.432	1.746
1.50	1.990	1.020	0.872	1.017	0.901	1.082
1.65	1.501	0.566	0.451	0.599	0.372	0.630
1.80	1.145	0.268	0.186	0.329	0.103	0.332
1.95	0.885	0.093	0.031	0.060	0.007	0.145
2.10	0.694	−0.003	−0.050	−0.056	−0.080	0.033
2.25	0.551	−0.053	−0.084	−0.078	−0.112	−0.029
2.40	0.444	−0.072	−0.091	−0.076	−0.115	−0.059
2.55	0.361	−0.072	−0.084	−0.063	−0.102	−0.070
2.70	0.296	−0.069	−0.070	−0.042	−0.090	−0.069
2.85	0.244	−0.056	−0.056	−0.030	−0.071	−0.063
3.00	0.202	−0.044	−0.042	−0.017	−0.048	−0.053
3.15	0.167	−0.030	−0.031	−0.011	−0.040	−0.043
3.30	0.138	−0.025	−0.022	−0.007	−0.025	−0.034
3.45	0.114	−0.016	−0.015	−0.003	−0.014	−0.026
3.60	0.093	−0.008	−0.010	−0.001	−0.011	−0.019
3.75	0.076	−0.003	−0.007	0.000	−0.008	−0.014
3.90	0.062	0.002	−0.005	0.000	−0.005	−0.010
4.05	0.050	0.005	−0.003		−0.003	−0.007
4.20	0.040	0.005	−0.002		−0.002	−0.004
4.35	0.032	0.000	−0.001		−0.001	−0.003
4.50	0.025	0.001	−0.001		−0.001	−0.002
4.65	0.020	0.002	0.000		0.000	−0.001
4.80	0.015	0.002	0.000		0.000	−0.001

curve **f**. The agreement with the experimental data is very poor for this basis set, the predicted reciprocal form factor being much too flat. Although very good from the point of view of energy (only $0.04\,E_h$, i.e. 0.02%, from the Hartree-Fock limit for FHF^- [29]), this basis set gives poor $B^a(s)$ values. The effect of the basis set used for hydrogen is rather small; the reciprocal form factor of the FHF^- anion is dominated by the F^- contribution (compare curve **e** and **f**).

The curves of the reciprocal form factor for NaFHF are shown in Fig. 6; the curves **a** and **b** have the same meaning as above (i.e. superposition of noninteracting atoms and experimental $B^a(s)$, respectively). The effect of the quality of the basis set together with the size of the cluster used for the calculation is examined. Curve **c** was calculated using MIDI basis sets for Na^+ as well as for the FHF^- anion, whereas for curve **d** a McLean-Chandler (MC) basis set [30] was used for sodium and DH for hydrogen fluoride. The position of the minimum as well as its depth change towards the experimental curve. Using clusters consisting of three anions and three cations does not change the reciprocal form factor much in the case of the MIDI basis set (see curves **c** and **e**); the improvement is, however, significant for the better MC/DH basis sets. Still, only qualitative agreement can be obtained using clusters consisting of only three anions.

A comparison of experimental and theoretical data for NaN_3 is shown in Figure 7. The effect of the size of the cluster can be seen when comparing curve **c** and **d**, where the quality of the basis set was kept constant (MIDI). For the reciprocal form factors of the curves **e** and **f**, a mixed cluster consisting of three anions and three cations was used, with MIDI basis sets for sodium and azide in the case of curve **e** and MC (Na^+) and DH (N_3^-) for curve **f**. Only the last curve shows qualitative agreement with experimental data; the position of the minimum is correct, but not the depth.

Better agreement between theoretical and experimental $B^a(s)$ was reached for NaOCN, as can be seen from Figure 8. The curves **c** and **d** were obtained starting from the same basis set (MIDI); for curve **d**, clusters of three anions and cations were used. For the reciprocal form factors of the curves **e** and **f**, anions and cations were packed together. Best agreement is reached for curve **f**, where an MC basis set for Na^+ and DH for the anion was employed.

5. Conclusions

In the present paper a comparison of theoretical and experimental reciprocal form factors for isotropic samples with good qualitative agreement can be reported. The influence of the quality of the basis set upon the theoretical reciprocal form factor in comparison to the experimental data was discussed. Some differences between STO and GTO basis sets were noticed; with increasing quality of the basis set (energies approaching the Hartree-Fock limit) these differences become smaller. We found, however, the reciprocal form factor to be much more sensitive in estimating the quality of a basis set than the convergence energy. Basis sets with only slightly different energies can lead to completely different $B^a(s)$ values.

The size of the anion or cation cluster used had a smaller but still significant influence on the agreement between experimental and theoretical data. We performed such calculations for the systems with rhombohedral crystal structures. The interaction of anions and cations along the C_3-axes of the rhombohedral cell is, owing to the large distances between the ions (they range from 6.59 Å in LiFHF to 7.60 Å in NaN_3), negligible over this distance (no change in the shape of the $B^a(s)$ curve in the range of s values between 1.5 Å and 5.0 Å could be observed). Much more important are interactions in directions perpendicular to the C_3-axes. Good agreement between theory and experiment could be reached only when taking these interactions into account. Further studies on systems with linear triatomic anions (especially N_3^- and FHF^-) including directional measurements on single crystals and extended solid-state calculations are in progress.

[1] J. W. M. DuMond, Phys. Rev. **35,** 643 (1929).
[2] J. W. M. DuMond, Rev. Mod. Phys. **5,** 1 (1933).
[3] B. Williams (Ed.), Compton Scattering, McGraw-Hill, New York 1977.
[4] M. Bräuchler, S. Lunell, I. Olovsson, and W. Weyrich, Int. J. Quantum Chem. **35,** 895 (1989).
[5] R. O. Horenian, Diplomarbeit, Konstanz 1989.
[6] W. Hoth and G. Pyl, Z. Angew. Chem. **42,** 888 (1929).
[7] G. Jander and E. Blasius, Einführung in das anorganisch-chemische Praktikum, S. Hirzel Verlag, Stuttgart 1984.
[8] R. Belcher, A. M. G. MacDonald, and E. Parry, Anal. Chim. Acta **16,** 524 (1957).
[9] R. Kruh, K. Fuwa, and T. E. McEver, J. Amer. Chem. Soc. **78,** 4256 (1956).
[10] C. J. Ludman, T. C. Waddington, E. K. C. Pang, and J. A. C. Smith, J. Chem. Soc.: Faraday Trans. **73,** 1003 (1977).
[11] A. Scattergood, Inorg. Synth. **II,** 86 (1946).
[12] C. Duval, Anal. Chim. Acta **5,** 506 (1951).
[13] P. Bachmann, Dissertation, Darmstadt 1979.
[14] B. M. Haas, Diplomarbeit, Konstanz 1987.
[15] M. W. Schmidt, J. A. Boatz, K. K. Baldridge, S. Kosecki, M. S. Gordon, S. T. Elbert, and B. Lam, QCPE Bulletin **7,** 115 (1987).
[16] M. Dupuis, D. Spangler, and J. J. Wendoloski, NRCC Software Catalog, University of California, Berkeley, CA (1980).
[17] C. Pisani, R. Dovesi, and C. Roetti, Hartree-Fock ab initio Treatment of Crystalline Systems, Springer Verlag, New York 1988.
[18] C. Pisani and R. Dovesi, Int. J. Quantum Chem. **27,** 501 (1980).
[19] E. Clementi and C. Roetti, Atomic Data and Nuclear Data Tables **14,** 177 (1974).
[20] S. Huzinaga, J. Andzelm, M. Klobukowski, E. Radzio-Andzelm, Y. Sakai, and H. Tatewaki, Gaussian Basis Sets for Molecular Calculations, Elsevier, Amsterdam 1984.
[21] J. S. Binkley, J. A. Pople, and W. H. Hehre, J. Amer. Chem. Soc. **102,** 939 (1980).
[22] T. H. Dunning, Jr., and P. J. Hay, in: H. F. Schäfer III (Ed.), Methods of Electronic Structure Theory, Plenum Press, New York 1977.
[23] L. K. Frevel and H. W. Rinn, Acta Cryst. **15,** 286 (1962).
[24] G. E. Pringle and D. E. Noakes, Acta Cryst. **24,** 262 (1968).
[25] B. L. McGaw and J. A. Ibers, J. Chem. Phys. **39,** 2677 (1963).
[26] M. Bassière, C. R. Acad. Sci. Paris **206,** 1309 (1938).
[27] A. D. McLean and M. Yoshimine, Tables of Linear Molecule Wave Functions, IBM J. Res. Dev., Suppl. 1967.
[28] H. Kistenmacher, H. Popkie, and E. Clementi, J. Chem. Phys. **58,** 5627 (1973).
[29] E. Clementi and A. D. McLean, J. Chem. Phys. **36,** 745 (1962).
[30] A. D. McLean and G. S. Chandler, J. Chem. Phys. **72,** 5639 (1980).
[31] M. S. Gordon, J. S. Binkley, J. A. Pople, W. J. Pietro, and W. J. Hehre, J. Amer. Chem. Soc. **104,** 2797 (1982).